Simulation of Exhaust Line Noise Using FEM and TMM

Ze Zhou and **Diego Copiello**, Free Field Technologies, MSC Software Company, Mont-Saint-Guibert, Belgium

Noise from both intake and exhaust lines contributes significantly to total vehicle noise. To assess the acoustic performance of automotive intake and exhaust lines, both the airborne engine noise propagating through the interior air of the line (known as pipe noise) and the structure-borne noise radiated by the line's surface shell structure (shell noise) should be evaluated. This article describes the study of both pipe and shell noise of a complex exhaust line using a finite-element method (FEM), coupled with a transfer matrix method (TMM).

In automotive NVH, intake noise and exhaust noise are important contributors to total vehicle noise. Today, as engine noise is increasingly controlled with new technologies, intake and exhaust noise emerge and, as shown in Table 1, reach the same level as engine noise in the typical truck used as an example. As a consequence, both automotive OEMs and suppliers pay increasing attention to intake and exhaust noises.

Take the exhaust line composed of volumes and ducts shown in Figure 1. The entire line is composed of different components of complex volume, connected by different ducts with constant cross section.

When studying noise from such an exhaust line, two noise sources need to be considered:

- Pipe noise – airborne engine noise propagating through the interior air of the line and emitted from the line's outlet to the environment (see Figure 2).
- Shell noise – structure-borne noise radiated by the vibration of shell structure of different components in the exhaust line (see Figure 3).

Finite-Element Method

Numerical simulation methods play an increasingly important role in the study of both pipe noise and shell noise of exhaust lines in the NVH department of OEMs and auto suppliers. Among the numerous numerical acoustics methods, FEM offers an advantageous combination of modeling flexibility, computation efficiency and results accuracy. Acoustical FEM can be easily coupled with structural FEM, which is already well known to most structure analysts. The acoustical and structural coupling in the FEM environment is called vibro-acoustic FEM. Equation 1 shows the coupled vibro-acoustic FEM system equation.

The impedance matrix on the left side of the equation takes contributions from both the structure and the fluid acoustic domains with coupling terms between them. This impedance matrix is multiplied by the system unknowns (structure displacement and fluid acoustic pressure) to give the external excitation on the right-hand side of the equation:

$$\begin{bmatrix} K_s + i\omega D_s - \omega^2 M_s & C \\ \omega^2 C^T & K_a + i\omega D_a - \omega^2 M_a \end{bmatrix} \begin{pmatrix} u(\omega) \\ p(\omega) \end{pmatrix} = \begin{pmatrix} f_s(\omega) \\ f_a(\omega) \end{pmatrix} \quad (1)$$

Advanced direct FEM solvers, such as MUMPS,[1] allow solving this system efficiently. Today, with ever-progressing computation resources, a vibro-acoustic FEM model can reach millions of degrees of freedom (DOF), while computation time is always decreasing.

Compared to the boundary-element method (BEM), FEM allows modeling more complex physics of acoustics, such as supporting multiple fluid domains, convected acoustics (sound propagating in a mean flow) and effects of temperature gradients in a fluid medium on the acoustic propagation.

With today's available meshing technologies, the historical obstacle of volume meshing on FEM no longer exists. As a consequence of this, an increasing number of acoustical engineers are embracing FEM and relying on it for their daily product design work. The FEM-based acoustic simulation software Actran, developed by Free Field Technologies (FFT), an MSC Software company, has been successfully applied in numerous intake and exhaust noise projects.[2,3] In this article, we demonstrate the capabilities of Actran in predicting exhaust line noise on the public model shown in Figure 1.

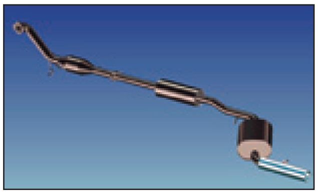

Figure 1. Exhaust line composed of volumes and ducts.

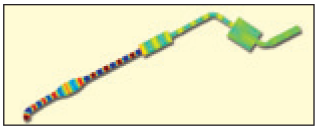

Figure 2. Pipe noise in exhaust system.

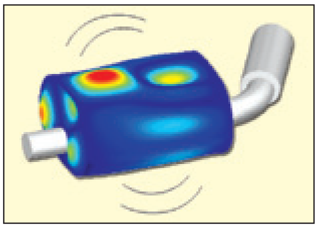

Figure 3. Shell noise in exhaust system.

Sound Transmission Loss

STL is the key indicator for acoustic performance related to pipe noise. One can numerically calculate the STL of a single component (for example, a muffler shown in Figure 4) or the STL of an entire exhaust line. The technique in both cases is the same and is explained in Figure 4. A (unit) incident acoustic power from upstream is applied at the inlet of the muffler. After sound propagation in the muffler, the transmitted power downstream is calculated at the muffler's outlet. The STL is defined as the logarithmic ratio between the incident and transmitted power (Equation 2). An acoustic non-reflective boundary condition is applied both at the outlet and inlet, to provide anechoic conditions for both propagating waves traveling downstream and any reflected waves traveling upstream. In Actran, analytical acoustic duct modes[4] are coupled with the FEM mesh both at the inlet and outlet to provide the excitation of incident power, the evaluation of transmitted power, and the non-reflective conditions.

$$TL = 10\log_{10}(W_{incident} / W_{transmitted}) \quad (2)$$

At a given frequency, a non-plane wave first occurs in larg-

Table 1. noise contributions of total truck vehicle noise (Source: SAE International).

Trucks	Engine Mechanical	Exhaust	Intake	Cooling Fan	Total Noise Level, dB(A)
1	81.0	84.0	75.0	82.0	88.0
2	81.0	84.0	75.0	82.0	88.0
3	83.0	86.0	80.0	81.0	89.0
4	85.0	82.0	80.0	83.0	89.0
5	83.0	83.0	72.0	78.5	87.0
6	81.0	77.0	70.0	82.0	85.5
7	82.5	86.0	79.0	82.0	89.5
8	85.0	82.0	80.0	83.0	89.0
9	83.0	83.0	72.0	78.5	87.0
10	81.0	77.0	70.0	82.0	85.5
11	83.5	82.5	74.0	78.0	87.0

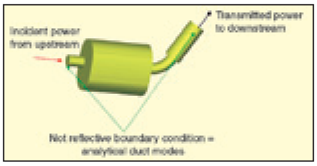

Figure 4. Sound transmission loss of muffler.

er volumes or in ducts with larger cross-sections. This is demonstrated in Figure 5. One observes a plane wave in the inlet and outlet ducts, but a non-plane wave in the muffler volume.

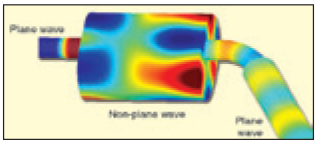

Figure 5. Non-plane (3D) wave occurs first in larger volume or ducts with large cross-section.

Transfer Matrix Method

TMM is an analytical method that allows assessing the STL of an entire exhaust line by combining acoustic transfer matrices of each of its constituent sub-components. Typically, a sub-component's transfer matrix is expressed in Equation 3, where I and R are the incident and transmitted waves for acoustic propagations in both directions (see Figure 6. Incident and transmitted waves in both directions in a subcomponent for its transfer matrix definition.).

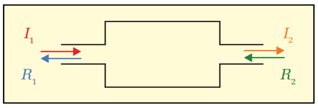

Figure 6. Incident and transmitted waves in both directions in a sub-component for its transfer matrix definition.

$$\begin{Bmatrix} I_1 \\ R_1 \end{Bmatrix} = \begin{bmatrix} \alpha & \beta \\ \gamma & \delta \end{bmatrix} * \begin{Bmatrix} I_2 \\ R_2 \end{Bmatrix} \quad \begin{bmatrix} \alpha & \beta \\ \gamma & \delta \end{bmatrix} = \text{Transfer matrix of the system} \tag{3}$$

The transfer matrix of an entire line T is assembled as the product of all the transfer matrices of its sub-components T_1, T_2, T_3, etc. as shown in Figure 7. Transfer matrix of entire line as a product of transfer matrices of its subcomponents..

A TMM utility is implemented in the Actran software. The transfer matrices of the sub-components are calculated individually using FEM. The combined FEM computation effort on all the sub-components is less than the total computation effort for the entire line. So in the study of exhaust noise, the combination of FEM and TMM offers both 3D capabilities for modeling pipe noise and shell noise and enhanced simulation efficiency.

Using TMM, the source amplitude and impedance can be plugged upstream to the entire line to calculate the sound pressure level transmitted from the outlet as shown in Figure 8. The source reflection factor is related to the source impedance by Equation 4:

$$Z = \rho c * \frac{1+r}{1-r} \Leftrightarrow r = \frac{Z - \rho c}{Z + \rho c} \tag{4}$$

The reflection factor depends on the nature of the source. For a source imposing acoustic pressure, the reflection factor is –1, meaning total pressure reflection with 180° phase change. For a source imposing acoustic velocity, the refection factor is 1, meaning total reflection without phase change. For a real source from the engine, the reflection factor could be frequency dependent, since the source tends to be a velocity source at low frequencies and pressure source at higher frequencies.

Perforation Simulation

Perforated plates are often used in muffler design. The acoustic propagation through the perforation can be simulated by meshing the holes of the perforation, as shown in Figure 9. A simpler, more efficient way to model perforation is to replace the mesh by an equivalent acoustic transfer admittance relation across the perforated plate as shown in Figure 10.

The transfer admittance matrix based on Mechel's formula is expressed by Equation 5. V_n and p are normal acoustic velocity and pressure on both sides of the perforation as shown in Figure 11. The assumption of Mechel's formula is $V_{n1} = V_{n2}$. Under such assumption, the calcualted admittance (A_p) is expressed in Equation 6. The different terms in Equation 6 are explained in Figure 12. Among these terms, the correction factor is determined by the the perforation pattern of the holes. Figure 13 provides the correction factor equations for hole patterns with square layout and hexagonal layout.

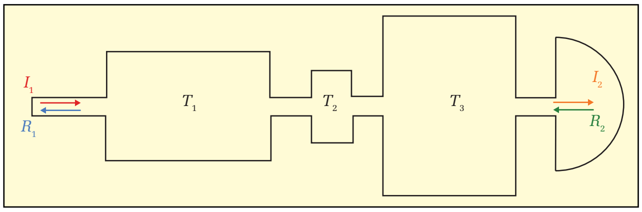

Figure 7. Transfer matrix of entire line as a product of transfer matrices of its subcomponents.

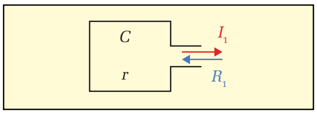

Figure 8. Source characterized by amplitude (C) and reflection factor (r).

$$\begin{bmatrix} v_{n1} \\ v_{n2} \end{bmatrix} = \begin{bmatrix} A_p & -A_p \\ -A_p & A_p \end{bmatrix} \begin{bmatrix} p_1 \\ p_2 \end{bmatrix} \tag{5}$$

$$A_p = 1/\left(R_p + j.X_p\right)$$

$$R_p = \frac{1}{\varepsilon}\sqrt{16\pi f \eta \rho_0}\left(1 + \frac{1}{2a}\right) \tag{6}$$

$$X_p = \frac{2}{\varepsilon}\pi f \rho (l + 2\Delta l)$$

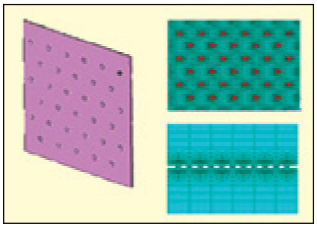

Figure 9. Acoustic meshing of a perforated plate.

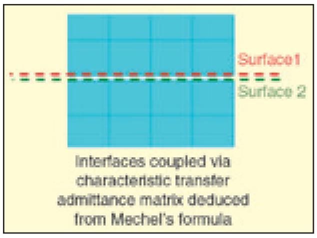

Figure 10. Equivalent acoustic transfer admittance across perforation.

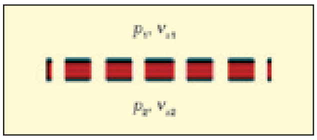

Figure 11. Normal acoustic velocity and pressure on two sides of perforation.

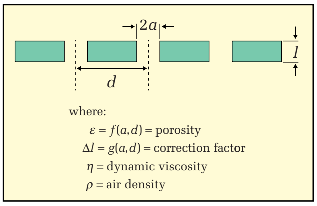

Figure 12. Explanation of different terms in calculating transfer admittance.

Porous Material Simulation

A porous material is usually used in muffler design to provide acoustic absorption to sound traveling through the muffler. In Actran, the porous material can be modeled using the Biot formulation. To model the porous-elastic behavior, the complete set of Biot properties need to be provided, including:

- Fluid properties – density, compressibility, viscosity, thermal conductivity, specific heat values
- Elastic parameters – solid density, Young's modulus, Poisson ratio
- Fluid-skeleton properties – porosity, flow resistivity, tortuosity, etc.
- Micromodel parameters – viscous length, thermal length

Simplified porous formulations, requiring fewer properties of porous material, are also available. The most well-known simplifications are the rigid porous formulation assuming rigid skeleton; the lumped porous formulation assuming extremely soft but heavy skeleton; and the empirical models such as Delany-Bazley porous model and the Miki porous model.[5,6]

Effects of Flow and Temperature Gradient

During sound propagation across ducts and mufflers, the non-uniform background flow modifies the propagation. The governing equation for this sound propagation is the convected Helmholtz equation.

The temperature gradient in the propagating medium changes the local air density and acoustic wave length and therefore modifies the sound propagation. In a FEM model, effects of flow and temperature can be taken into account by defining flow speed and temperature values on each FEM node.

Numerical Examples

STL of Muffler. STL is calculated for the muffler components in

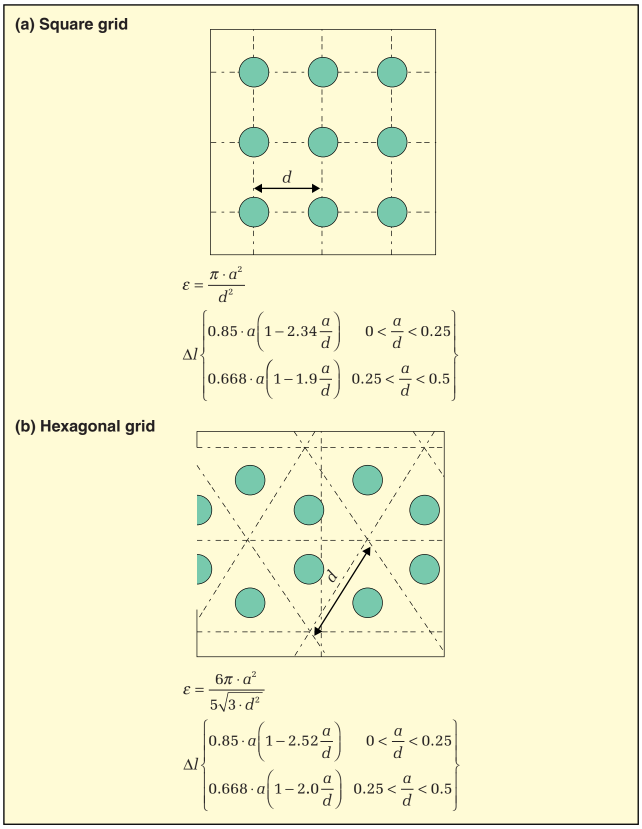

Figure 13. Correction factor of perforation transfer admittance; square grid (top) and hexagonal grid (bottom).

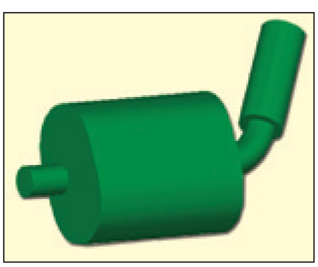

Figure 14. Expansion chamber of baseline muffler.

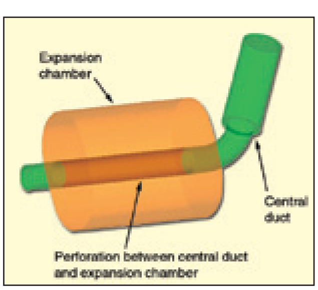

Figure 15. Muffler with perforation.

the exhaust line. Five configurations are compared:

- Baseline muffler, which is the expansion chamber shown in Figure 14.
- Muffler with perforation, separating the central duct and the expansion chamber shown in Figure 15.
- Muffler with perforation and porous material fill in the expansion chamber; the porous material is modeled using rigid porous formulation.
- Muffler with perforation, porous material, and flow effect shown in Figure 16.
- Muffler with perforation, porous material, and temperature effect shown in Figure 16.

The STL curves of different configurations are shown in Figure 17. In the baseline muffler, under 500~600 Hz, the sound propagation has a 1D planar behavior. As the frequency increases, 3D behavior occurs. The perforated sheet changes the STL of the baseliner muffler, but not significantly. When the porous material is added to the expansion chamber, the STL curve becomes much smoother, with increased levels in the higher frequency range. The effect of flow and temperature gradients are relatively important.

Muffler Shell Noise. The shell noise caused by muffler shell vibration is calculated using a two-step approach. In the first step, the coupled problem of interior air and muffler shell is calculated. The shell vibration is obtained, as shown in Figure 18. In the same figure, the infinite elements allowing the shell noise radiation and the far-field virtual microphones are shown. The sound pressure level directivity around the microphone circle at 500 and 1000 Hz is shown in Figure 19.

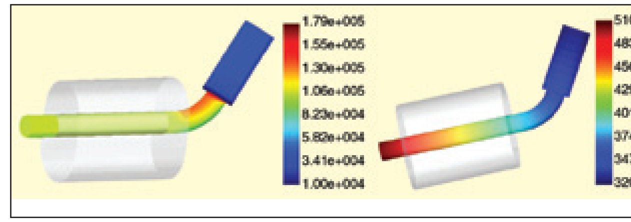

Figure 16. Flow speed in central duct, in mm/s ((left); temperature in central duct, in K (right).

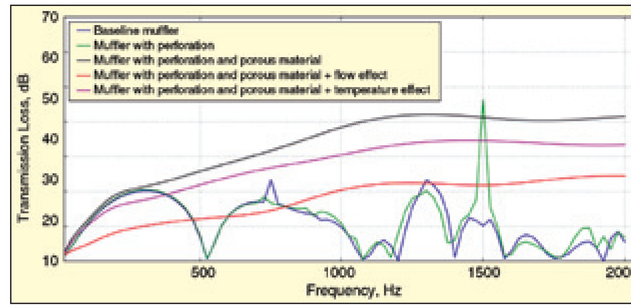

Figure 17. Sound transmission loss of different muffler models.

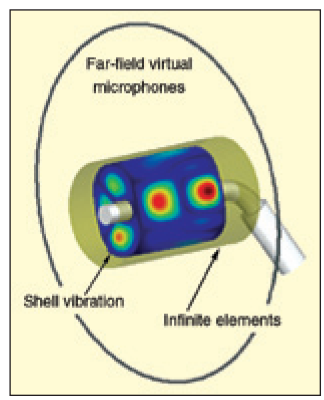

Figure 18. Shell vibration at 1000 Hz, infinite elements and virtual microphones.

Entire Exhaust Line Modeling and TMM. The entire line is composed of three different acoustic volumes, connected by ducts. The third volume is the muffler studied in the previous section. Here, the muffler has the perforated sheet but no porous material in the expansion chamber.

The transmitted power is computed at the outlet with free-field radiation conditions, provided by Inifnite Elements, and shown in Figure 20. We observe in the same figure that the free-field outlet condition generates acoustic reflection, as a duct section change occurs connecting the finite cross-section with the free-field infinite cross section.

The acoustic pressure at 2000 Hz is shown in Figure 21. One observes 1D sound propagation behavior in the ducts and in the first two volumes. In the third volume, 3D behavior occurs.

In the TMM model, the exhaust line is divided into four subcomponents corresponding to the three acoustic volumes and the free-field outlet condition shown in Figure 22. Figure 23 shows a perfect correlation of STL curves calcualted on the entire line model (frequency step = 50 Hz) and on the model employing the TMM technique (frequency step = 100 Hz), respectively.

Computation Statistics. The acoustic mesh contains about 2 million nodes for the entire line in a single FEM model valid up to 2000 Hz. The calculation time with the Actran solver is one hour per frequency on a standard workstation (the RAM requirement is 20 GB). Using TMM and solving the line sub-components separately, the computation time per frequency is reduced to 30 minutes, and the RAM consumption is reduced to 10 GB (required by the largest sub-component – the muffler volume). Using frequency parallelization, the computation time per frequency can be divided by the number of parallel processes.

Plugging Engine Source to TMM. The TMM is coupled with a unit-source amplitude with three reflection factors (0, –1 and 1) to calculate the SPL at a virtual microphone 1 m away from the outlet. The SPL results with up to 2000 Hz and a frequency step of 100 Hz are shown in Figure 24.

Conclusions

We presented a complex exhaust noise problem in this article. The complexity was related to many factors, namely the irregular

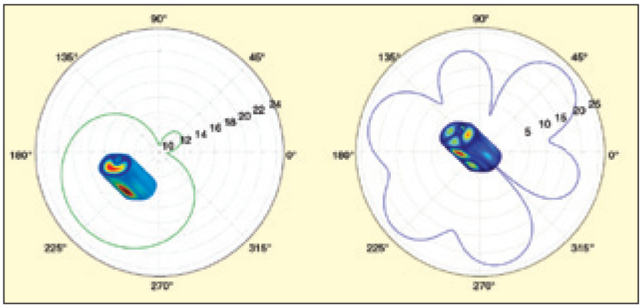

Figure 19. Far-field directivity at 500 Hz (left) and 1000 Hz (right).

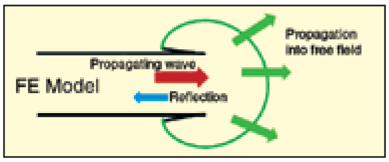

Figure 20. Infinite elements at outlet allowing free-field radiation.

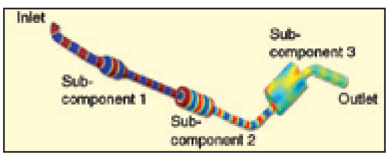

Figure 21. Acoustic pressure in exhaust line at 2000 Hz.

geometry, the presence of both a perforated sheet and porous material, and a non-uniform flow involving both convection and temperature gradients. This article demonstrates the numerical simulation of such complex exhaust line noise using FEM and TMM, both available in the Actran software.

References

1. MUMPS Solver: http://mumps.ensaeeiht.fr/.
2. Mitsubishi Motors, "Exhaust System Modeling Using a Transfer Matrix Method Coupled to Actran," Actran Users Conference, Belgium, 2010.
3. T. Le Bourdon, *et al.*, "Vibro-Acoustic Simulation of Intake Air Filter Using a Hybrid Modal Physical Coupling," ISNVH 2012-01-1549.
4. Analytical Duct Modes: J. M. Tyler and T. G. Sofrin, "Axial Flow Compressor Noise Studies," SAE Transactions, Vol. 70, pp. 309-332, 1962.
5. M. E. Delany and E. N. Bazley, "Acoustical Characteristics Of Fibrous Absorbent Materials," Report of the National Physical Laboratory, Aerodynamics division, March 1969.

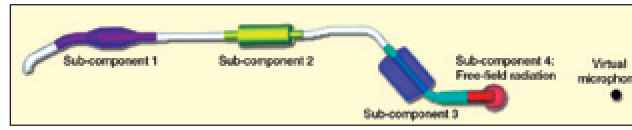

Figure 22. Transfer matrix method components.

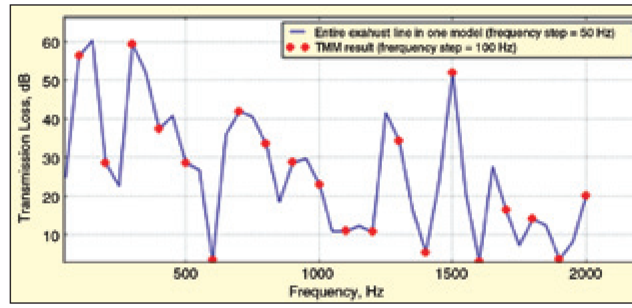

Figure 23. Sound transmission loss of entire exhaust line.

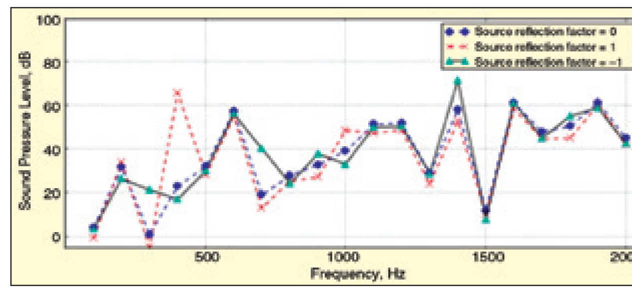

Figure 24. Sound pressure level on exterior microphone due to unit source with different reflection factors.

6. Y. Miki, "Acoustical Properties of Porous Materials – Modifications of Delany-Bazley Models," *J. Acoust. Soc. Jpn.* 11(1), pp. 19-24 1990. SV

The author may be reached at: ze.zhou@fft.be.